Locally Monotonic Diffusion

Scott T. Acton, *Senior Member, IEEE*

***Abstract*—Anisotropic diffusion affords an efficient, adaptive signal smoothing technique that can be used for signal enhancement, signal segmentation, and signal scale-space creation. This paper introduces a novel partial differential equation (PDE)-based diffusion method for generating locally monotonic signals. Unlike previous diffusion techniques that diverge or converge to trivial signals, *locally monotonic (LOMO) diffusion* converges rapidly to well-defined LOMO signals of the desired degree. The property of local monotonicity allows both slow and rapid signal transitions (ramp and step edges) while excluding outliers due to noise. In contrast with other diffusion methods, LOMO diffusion does not require an additional regularization step to process a noisy signal and uses no *ad hoc* thresholds or parameters. In the paper, we develop the LOMO diffusion technique and provide several salient properties, including stability and a characterization of the root signals. The convergence of the algorithm is well behaved (nonoscillatory) and is independent of signal length, in contrast with the median filter. A special case of LOMO diffusion is identical to the optimal solution achieved via regression. Experimental results validate the claim that LOMO diffusion can produce denoised LOMO signals with low error using less computation than the median-order statistic approach.**

***Index Terms*—Anisotropic diffusion, partial differential equations, scale space, signal enhancement.**

I. Introduction

DIFFUSION processes may be used to model a special class of nonlinear adaptive signal filters. The same approach used to solve heat diffusion and bacteria migration problems [8] can be applied to the adaptive processing of a digital signal for the purposes of signal enhancement or feature extraction, for example. The localized diffusion operation can be modeled by a system of partial differential equations (PDE's) that depend only on limited signal neighborhoods.

The PDE-based signal diffusion methods are attractive for several reasons. Important signal features such as edges can be preserved using the diffusion approach; an anisotropic diffusion algorithm [1], [9] can be designed that enacts intraregion smoothing as opposed to interregion smoothing. The diffusion PDE's generate a signal *scale space* [14]. The resultant family of signals that vary from coarse to fine may be used in several multiscale signal analyses such as hierarchical searches, segmentation, and coding. Unlike scale spaces generated using linear filters (see Fig. 1), anisotropic diffusion can generate a scale-space where edge localization is preserved (see Fig. 2). From an implementation perspective, the simple PDE's can be efficiently executed on a locally connected parallel processor.

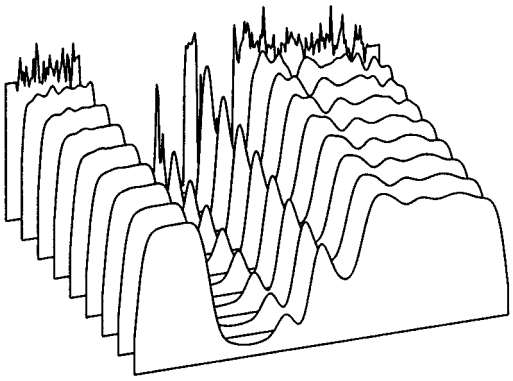

Fig. 1. Scale space generated by the Gaussian filter. From back to front: original noisy input signal ($N = 256$); results of successive convolution with a Gaussian filter (standard deviation $\sigma = 4$).

Caselles *et al.* provide additional motivation for exploring PDE-based signal processing [4]. The PDE methods use simple models in the continuous domain where discrete filters become PDE's as the sample spacing goes to zero. The simplified formalism allows various properties to be proved or disproved including stability, locality, and causality. In addition, the analysis allows discussion of the existence and uniqueness of solutions. High degrees of accuracy and stability are possible through the mature results of numerical analysis. Finally, the PDE approach facilitates the combination of algorithms through the weighted sum of PDE's.

In a typical PDE approach, we have some knowledge of the dynamics of a physical process, and we model the dynamics with a suitable PDE. However, in the case pursued in this paper, we know the physical characteristics of the solution, and we design PDE's that converge to signals with the appropriate properties. With the basic premise that we wish to preserve step edges (abrupt signal transitions), ramp edges, and smooth regions while eliminating impulses (noise), we can describe the prototypical signal with the property of *local monotonicity*.

Previous diffusion algorithms have been shown to diverge, to converge to constant signals, or to converge to piecewise constant signals [3], [16]. Although these results are important to the understanding the current diffusion algorithms, the resultant signals may not be desired in applications where preservation of ramp edges is important. Diffusion algorithms that diverge [9] or converge to signals of zero mean curvature [15] must be halted in progress to obtain a nontrivial signal. The stopping conditions are difficult to estimate and do not provide a guaranteed description of the final signal characteristics. Piecewise constant signals, on the other hand, may be of interest in

Manuscript received May 28, 1998; revised November 18, 1999. This work was supported in part by the U.S. Army Research Office under Grant DAAH04-95-1-0255 and by NASA under EPSCoR Grant NCC5-171. The associate editor coordinating the review of this paper and approving it for publication was Prof. Arnab K. Shaw.

The author is with the School of Electrical and Computer Engineering, Oklahoma State University, Stillwater, OK 74078-0321 USA (e-mail: sacton@ceat.okstate.edu).

Publisher Item Identifier S 1053-587X(00)03302-X.

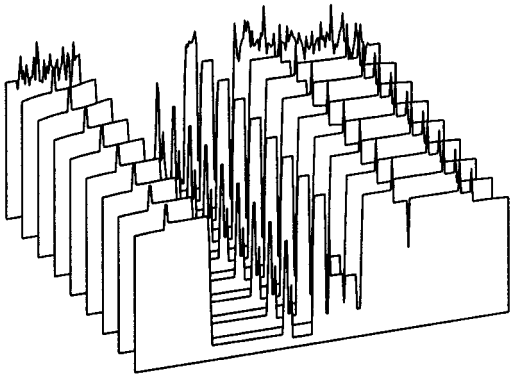

Fig. 2. Scale space generated by standard anisotropic diffusion using (5) (with $k = 10$) [9]. From back to front: original noisy input signal ($N = 256$); signals generated by diffusing the original signal with the same number of iterations used in generating the corresponding LOMO diffusion result in Fig. 3.

two special circumstances. If the original (uncorrupted) signal is piecewise constant in a denoising application or if the desired result of processing is a piecewise constant segmentation, diffusion to a piecewise constant signal may be appropriate. However, the piecewise constant model is not generalized; this may be noted particularly in the cases where slow transitions in signal intensity (or ramp edges) should be preserved in processing. The current anisotropic diffusion algorithms that do converge to piecewise constant signals are also limited by the use of an edge threshold and by the inability to control spatial feature scale directly. For example, the algorithm used in [3] achieves a fixed-point solution for piecewise constant signals where "all discontinuities are above a threshold." It is our viewpoint that feature scale (not the relative difference between features in intensity) should influence the rejection or preservation of the feature in signal diffusion. In terms of scale, the current piecewise constant approaches do not allow the specification of feature size, which is a critical aspect of generating a scale-space for multiscale signal processing. Define a signal to be piecewise constant of degree d (PICO-d) if each sample is a member of a constant (contiguous) interval of at least length d. Since all signals are PICO-1, it is clear that not all PICO signals are of interest; the degree of piecewise constancy cannot be specified with current implementations of signal diffusion. Here, we describe a diffusion algorithm that converges to a more generalized model that allows step and ramp transitions, does not depend on a gradient magnitude threshold, and allows control of feature scale.

One qualitative characteristic desired in PDE-based diffusion is signal smoothness. For discrete signals, the traditional notion of evaluating smoothness by continuity does not apply. Moreover, limiting the instantaneous rate of change in a signal (with a gradient magnitude threshold) leads to destruction of the signal edges. Locally monotonic (LOMO) signals are nonincreasing or nondecreasing within all intervals of a specified length. Local monotonicity does not limit the rate of change in signal but instead limits the rate of signal oscillation. The smoothness of a digital signal can be quantified by its *lomotonicity*, which is the highest *degree* of local monotonicity possessed by the signal [10].

Definition 1: A length-N signal $\boldsymbol{I}$ is locally monotonic of degree d (or LOMO-d) if it is monotonic (nondecreasing or nonincreasing) within each interval of length d [e.g., $\{I(x), I(x+1), \cdots, I(x+d-1)\}$].

Every digital signal is LOMO-2, and a globally monotonic signal would be LOMO-N: the highest degree possible. Note that LOMO-d signals are not, in general, globally monotonic. A LOMO-d signal may be partitioned into nonincreasing ramps, nondecreasing ramps, and constant sections (of length $d-1$ or greater). Therefore, in a LOMO signal, increasing and decreasing ramps are separated by constant plateaus of length $d-1$ or greater. The degree of local monotonicity provides an effective description of signal scale that allows a causal scale-space: one in which new features are not created with increasing scale. It is worthwhile to note that for $d > e$, a LOMO-d signal is also LOMO-e.

The concept of local monotonicity first appeared in the analysis of the root signals produced by the median filter [6]. Since that time, algorithms have been designed that directly generate locally monotonic signals via nonlinear regression [10], [12]. In the regression approach, the computation of a LOMO signal that resembles the original (and possibly noisy) signal is treated as a combinatorial optimization problem. This paper investigates the generation of LOMO signals via a simple adaptive diffusion mechanism. The PDE-based method has advantages over the median filter roots in computational complexity while maintaining closeness to the original signal. Furthermore, LOMO diffusion is not subject to the pathological behavior of the median filter given oscillating signals as input [6]. Compared with the regression-based solutions, LOMO diffusion has advantages in computational cost.

A major contribution of the LOMO diffusion technique is the convergence to a nontrivial class of signals. In addition, two other problems that are found with current diffusion algorithms are solved by LOMO diffusion. First, the LOMO diffusion technique provides a method to describe the resultant signal scale from its lomotonicity. In other words, LOMO diffusion defines a practical signal scale-space in which feature scale may be exactly specified. Previous "scale aware" approaches [5], [11] use prefiltering to eliminate small scale objects such as outliers due to noise. Second, since the property of local monotonicity does not define edges simply by large gradient magnitude, LOMO diffusion does not require the *ad hoc* edge threshold that is found in most diffusion implementations [1], [9], [16].

II. Theory

A. Anisotropic Diffusion

Given a signal $\boldsymbol{I}$ defined on a continuous domain $X \in \Re$, the following PDE may be used to perform the diffusion operation:

$$\frac{\partial I(X)}{\partial t} = \text{div}[c(X)\nabla I(X)] \tag{1}$$

where $c(X)$ is the diffusion coefficient at location X that inhibits or encourages diffusion, and the time parameter t is often

related to scale. This PDE can be discretized by the following Jacobi (simultaneous update) iterate:

$$[I(x)]_{t+1} \leftarrow \{I(x) + \Delta T[c_w(x)\nabla I_w(x) + c_e(x)\nabla I_e(x)]\}_t \tag{2}$$

where ΔT is the time step, and t represents the number of iterations. Henceforth, the domain for $\boldsymbol{I}$ is restricted to finite length discrete signals where $0 \leq x \leq N-1$, and $x \in \boldsymbol{Z}$. $\nabla I_w(x)$ and $\nabla I_e(x)$ are the simple differences with respect to the "western" and "eastern" neighbors, respectively, and are defined by

$$\nabla I_w(x) = I(x - h_w) - I(x) \tag{3}$$

and

$$\nabla I_e(x) = I(x + h_e) - I(x). \tag{4}$$

The parameters h_e and h_w define the sample spacing used to estimate the directional derivatives and are restricted to the set of cardinal numbers: $h_e, h_w \in \{1, 2, 3, \cdots\}$. Although typical discretizations employ unity-width sample spacings for difference operations, these parameters will be varied here to produce locally monotonic signals of the desired degree.

The diffusion coefficient is generally a smooth, nonincreasing function of image gradient magnitude. A typical exponential form is [9]

$$c_p(x) = \exp\left\{-\left[\frac{\nabla I_p(x)}{k}\right]^2\right\} \tag{5}$$

where k is a gradient magnitude threshold and determines which edges will be retained in the diffusion process, and p is the direction of diffusion (in this case, "e" or "w"). No analytical method exists to select k for a general class of signals, so k is usually selected in an *ad hoc* manner. Another problem associated with using this diffusion coefficient is the preservation of outliers due to noise. Because the outliers (and other small features) may have large gradient magnitudes, they are protected in the diffusion process. The preservation of these outliers and detailed features leads to the inability to generate a scale space, where the features in the signals vary from coarse to fine. Although the scale-space generated by anisotropic diffusion with (5) in Fig. 2 is clearly superior in terms of edge preservation to the Gaussian scale space of Fig. 1, the anisotropic diffusion algorithm is not superior in terms of removing impulse noise.

To correct this limitation, new diffusion coefficients have been proposed [5] that use a presmoothed image to regularize the diffusion. This approach, however, introduces a linear diffusion process into the nonlinear diffusion process, limiting edge retention and localization. A more recent attempt to improve the scale-space generation ability of diffusion is given in [11]. Here, a morphological prefilter is used to eliminate small features. While maintaining edge localization, the morphological diffusion approach still contains the ambiguous edge threshold parameter.

Instead of fixing the traditional anisotropic diffusion approach via a regularizing filter, we choose to design a diffusion technique that converges to a signal in which feature scale is explicitly specified.

B. Locally Monotonic Diffusion

To create a discretized PDE that generates digital LOMO signals, it may be observed that local monotonicity is closely related to the sign skeleton of the difference signal. For a signal $I(x)$, the sign skeleton $S(x)$ is computed by $S(x) = \text{sgn}[I(x+1) - I(x)]$ for $0 \leq x \leq N-2$. Within a given signal interval, if both negative and positive values exist in $S(x)$, that interval is not monotonic. The goal of the LOMO PDE may be conceptualized as removing opposite signs in the sign skeleton locally. For digital signals, this goal is satisfied by reducing local differences between samples to zero. Oscillatory regions of the signal are thereby "flattened" to produce local monotonicity. The diffusion algorithm essentially removes the *nonmonotone points* and preserves the *monotone points*, where the definition of these points is given below.

Definition 2: Given a subsequence $\{I(x-h_w), I(x), I(x+h_e)\}$, let $I(x)$ be defined as a *monotone point* if $I(x-h_w) \leq I(x) \leq I(x+h_e)$ or $I(x-h_w) \geq I(x) \geq I(x+h_e)$. $I(x)$ is therefore a positive-going *nonmonotone point* if $I(x) > I(x-h_w)$ and $I(x) > I(x+h_e)$. It is a negative-going nonmonotone point if $I(x) < I(x-h_w)$ and $I(x) < I(x+h_e)$.

A PDE that limits the sign changes of pixel differences within a local neighborhood, removing nonmonotone points, may be designed using the following diffusion coefficient:

$$c_p(x) = \frac{1}{|\nabla I_p(x)|}. \tag{6}$$

Then, the discrete diffusion update (2) becomes

$$[I(x)]_{t+1} \leftarrow (I(x) + (1/2)\{\text{sgn}[\nabla I_w(x)] + \text{sgn}[\nabla I_e(x)]\})_t \tag{7}$$

where a maximum time step (for stability) of $\Delta T = 1/2$ is used.

With the restriction that the diffusion coefficient must be a smooth and nonincreasing function of gradient magnitude, we must modify the difference terms for the case where either simple difference $\nabla I_e(x)$ or $\nabla I_w(x)$ is zero. Let $\nabla I_w(x) \leftarrow -\nabla I_e(x)$ in the case of $\nabla I_w(x) = 0$; $\nabla I_e(x) \leftarrow -\nabla I_w(x)$ when $\nabla I_e(x) = 0$. The case where $\nabla I_w(x) = \nabla I_e(x) = 0$ produces no change in (7) and does not need to be modified.

In order to accommodate two special cases in which convergence is prolonged (not precluded), we provide an enhanced diffusion update based on the original diffusion update in (7). The first special case is an "overshoot" of one intensity level. In the event where $I(x)$ and $I(x-h_w)$ are nonmonotone points and $\nabla I_w(x) = 1$, an overshoot of one intensity level will occur with the update according to (7); the new values of $I(x)$ and $I(x-h_w)$ will pass each other instead of becoming equal, as desired. The same case can occur with $I(x)$ and $I(x+h_e)$. Note that these overshoots can occur when $h_e = h_w$ or when $h_e \neq h_w$. The second problem occurs only when $h_e \neq h_w$. This problem may be described as a "lag." When $I(x)$ is equal to $I(x+h_e)$ [or $I(x-h_w)$], and $I(x+h_e)$ [or $I(x-h_w)$] changes to make $I(x)$ a nonmonotone point, $I(x)$ will follow $I(x+h_e)$ [or $I(x-h_w)$], lagging behind by one intensity level. This lag will delay convergence.

An update that avoids both the overshoot problem and the lag problem is given by

$$[I(x)]_{t+1} \leftarrow (I(x) + (p(x)/2)\{\text{sgn}[\nabla I_w(x)] + \text{sgn}[\nabla I_e(x)]\} + a(x))_t \quad (8)$$

where $p(x)$ handles the overshoot case, and $a(x)$ handles the lag case. In (8), $p(x) = 1_{[l(x)]'}$, where $1_{(\cdot)}$ is the indicator function. Therefore, diffusion is inhibited when the expression $l(x)$ is true. The signal values affected by the overshoot problem are termed *opposite-going single-difference* (OGSD) points. Position $x-h_w$ is an opposite-going single difference point with respect to (w.r.t.) position x if the difference between the values of $I(x-h_w)$ and $I(x)$ is unity, and one of them is a positive-going nonmonotone point, whereas the other is a negative-going nonmonotone point. This relationship is quantified by the following Boolean expression:

$$\begin{aligned} o(x, x-h_w) = &\{[\nabla I_w(x) = 1] \wedge [\nabla I_{ww}(x) < 0] \\ &\wedge [\nabla I_{we}(x) < 0] \wedge [\nabla I_e(x) > 0]\} \\ &\vee \{[\nabla I_w(x) = -1] \wedge [\nabla I_{ww}(x) > 0] \\ &\wedge [\nabla I_{we}(x) > 0] \wedge [\nabla I_e(x) < 0]\} \end{aligned} \quad (9)$$

where

$$\begin{aligned} \nabla I_{ww}(x) &= I(x-2h_w) - I(x-h_w) \\ \nabla I_{we}(x) &= I(x-h_w+h_e) - I(x-h_w) \\ \nabla I_{ee}(x) &= I(x+2h_e) - I(x+h_e) \end{aligned}$$

and

$$\nabla I_{ew}(x) = I(x+h_e-h_w) - I(x+h_e).$$

Note that for $x < 2h_w$, $\nabla I_{ww}(x) = 0$, and for $x > N-2h_e-1$, $\nabla I_{ee}(x) = 0$. Similarly, $x+h_e$ is an opposite-going single difference point w.r.t. position x if the following expression is asserted:

$$\begin{aligned} o(x, x+h_e) = &\{[\nabla I_e(x) = 1] \wedge [\nabla I_{ew}(x) < 0] \\ &\wedge [\nabla I_{ee}(x) < 0] \wedge [\nabla I_w(x) > 0]\} \\ &\vee \{[\nabla I_e(x) = -1] \wedge [\nabla I_{ew}(x) > 0] \\ &\wedge [\nabla I_{ee}(x) > 0] \wedge [\nabla I_w(x) < 0]\}. \end{aligned} \quad (10)$$

Then, diffusion is inhibited when $I(x)$ has an OGSD point that does not have any OGSD points or when $I(x)$ has an OGSD point and is lower in value than the OGSD value

$$\begin{aligned} l(x) = &o(x, x-h_w) \wedge ([I(x) < I(x-h_w)] \\ &\vee [o(x-h_w, x-h_w+h_e)]' \\ &\wedge\ [o(x-h_w, x-2h_w)]') \\ &\vee o(x, x+h_e) \wedge ([I(x) < I(x+h_e)] \\ &\vee [o(x+h_e, x+h_e-h_w)]' \\ &\wedge\ [o(x+h_e, x+2h_e)]') \end{aligned} \quad (11)$$

where $[\,]'$ represents the complement operation in the Boolean expression. Note that when $h_e = h_w$, if $I(x-h_w)$ is an OGSD point w.r.t. $I(x)$, then $I(x)$ is an OGSD point w.r.t. $I(x-h_w)$. The same holds for $I(x)$ and $I(x+h_e)$ when $h_e = h_w$. In the case where $h_e \neq h_w$, $I(x)$ and $I(x+h_e)$ [or $I(x)$ and $I(x-h_w)$] do not have the same codependence.

The additional term $a(x)$ in (8) prevents the lag scenario. In this case, the change in $I(x)$ is set to the projected change (at time $t+1$) in $I(x-h_w)$ [which is termed $\nabla_t(x-h_w)$] if the condition $C_w(x)$ is met. Likewise, the change in $I(x)$ is set to the change in $I(x+h_e)$, $\nabla_t(x+h_e)$, if the condition $C_e(x)$ holds. $C_w(x)$ is given by

$$\begin{aligned} C_w(x) = &[I(x) = I(x-h_w)] \\ &\wedge \begin{pmatrix} \{[I(x) > I(x+h_e) + \nabla_t(x+h_e)] \\ \quad \wedge [\nabla_t(x-h_w) = -1]\} \\ \quad \vee \{[I(x) < I(x+h_e) + \nabla_t(x+h_e)] \\ \quad \wedge [\nabla_t(x-h_w) = 1]\} \end{pmatrix} \end{aligned} \quad (12)$$

and $C_e(x)$ is given by

$$\begin{aligned} C_e(x) = &[I(x) = I(x+h_e)] \\ &\wedge \begin{pmatrix} \{[I(x) > I(x-h_w) + \nabla_t(x-h_w)] \\ \quad \wedge [\nabla_t(x+h_e) = -1]\} \\ \quad \vee \{[I(x) < I(x-h_w) + \nabla_t(x-h_w)] \\ \quad \wedge [\nabla_t(x+h_e) = 1]\} \end{pmatrix} \\ &\wedge [C_w(x)]'. \end{aligned} \quad (13)$$

Thus, the antilag term is expressed as

$$a(x) = \nabla_t(x-h_w)1_{C_w(x)} + \nabla_t(x+h_e)1_{C_e(x)}. \quad (14)$$

Here, we assume that (11) and the projected changes for time $t+1$ are computed before (14). Note that both $C_e(x)$ and $C_w(x)$ cannot be true simultaneously; therefore, the maximum update change is still bounded by a single intensity level change.

While the enhancements given in (8)–(14) prevent the occurrences of overshoot and lag, the original update in (7) is sufficient for practical implementation. Aside from synthetically derived pathological signals containing a string of interdependent points that produce overshoots and lags, the update given in (7) provides equivalent solution quality without a significant sacrifice in computational expense (in terms of the number of updates), as compared with the update of (8). In fact, with the 200 signals used in the results (see Section IV), the overall number of diffusion updates was equal using both (7) and (8). Nevertheless, in order to provide absolute proofs of convergence, the enhanced update of (8) is utilized in the analysis (see Section III).

Definition 3: The *LOMO diffusion update* function is given by (8) with $\nabla I_w(x) \leftarrow -\nabla I_e(x)$ when $\nabla I_w(x) = 0$ and $\nabla I_e(x) \leftarrow -\nabla I_w(x)$ when $\nabla I_e(x) = 0$. Each $I(x)$ in $\boldsymbol{I}$ is updated simultaneously for $\forall x$: $h_w \le x \le N - h_e - 1$.

In the analysis, we will show that the LOMO diffusion PDE's converge to a root signal. Let $ld(\boldsymbol{I}, h_w, h_e)$ represent the root signal produced by (8) [or by (7)] with input $\boldsymbol{I}$ for discrete spacing h_w and h_e. Multiple passes of this diffusion operation can yield the LOMO signal of the desired degree. Let $ld_d(\boldsymbol{I})$

denote the LOMO diffusion sequence that gives a LOMO-d (or greater) signal from input $\boldsymbol{I}$. For odd values of $d = 2m + 1$

$$ld_d(\boldsymbol{I}) = ld(\cdots ld(ld(ld(\boldsymbol{I}, m, m), m-1, m) \\ m-1, m-1)\cdots, 1, 1). \quad (15)$$

In (15), the process commences with $ld(I, m, m)$ and continues with spacings of decreasing widths until $ld(I, 1, 1)$ is implemented. For even values of $d = 2m$, the sequence of operations is similar:

$$ld_d(\boldsymbol{I}) = ld(\cdots ld(ld(ld(\boldsymbol{I}, m-1, m) \\ m-1, m-1), m-2, m-1)\cdots, 1, 1). \quad (16)$$

How does it work? The operation $ld(\boldsymbol{I}, h_w, h_e)$ converges to a signal in which each subsequence $\{I(x - h_w), I(x), I(x + h_e)\}$ is monotonic (see Theorem 1 in Section III). In order to generate a LOMO-d signal where $d = 2m + 1$, the subsequence representing the endpoints of the d-length intervals $\{I(x - m), I(x), I(x + m)\}$ is first forced to become monotonic. Then, subsequences of decreasing widths become monotonic via LOMO diffusion. Finally, $ld(\boldsymbol{I}, 1, 1)$ is executed, completing the process of making each d-length interval monotonic.

Although the multiple diffusion passes may appear to be expensive computationally, we can show by experiment and analysis that the number of iterations needed for convergence to a root signal is bounded. The problem of obtaining a LOMO-d signal (that resembles the initial signal) from a PDE in a minimum number of steps is still open, however. In fact, experiments show that less conservative sequences may be used to produce LOMO sequences of the same degree. For example, the sequence of $ld(\boldsymbol{I}, 4, 5)$ to $ld(\boldsymbol{I}, 3, 4)$ to $ld(\boldsymbol{I}, 2, 3)$ to $ld(\boldsymbol{I}, 1, 2)$ to $ld(\boldsymbol{I}, 1, 1)$ has been used successfully to generate LOMO-10 signals. On the average, this reduced sequence only lessened the computational load by a few iterations, however.

An advantage of LOMO diffusion is the ability to specify (exactly) the desired feature scale. In other words, if an application calls for removing all features of width less than d, a LOMO-d diffusion may be enacted. The Gaussian scale space is parameterized by the standard deviation of the Gaussian kernel, but the exact size of the features to be removed in filtering cannot be specified (see Fig. 1). LOMO diffusion is thus well suited for multiscale analysis. Examine the scale space created by LOMO diffusion in Fig. 3. Edges are retained, and noise/details are eliminated. Because the traditional anisotropic diffusion mechanism [9] inhibits diffusion where the local image gradient magnitude is high (relative to an *ad hoc* constant), impulses from noise are retained as well as edges (see the scale space in Fig. 2). Repetitive application of the median filter may also be used to generate a family of LOMO signals of desired degree as in Fig. 4. We will see, however, that the expense of the median filter is far greater than the PDE approach and that the median filter has difficulty with oscillating signals [see Fig. 5].

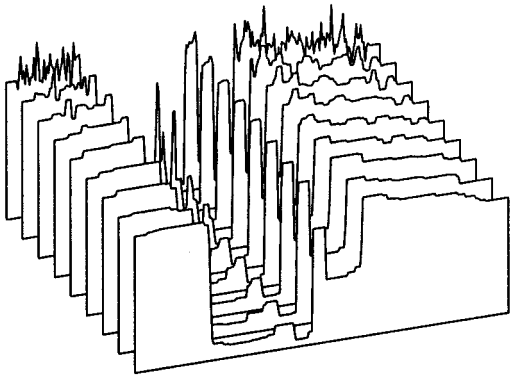

Fig. 3. Scale space generated by LOMO diffusion. From back to front: original noisy input signal ($N = 256$); LOMO-3 root signal; LOMO-4 root signal, $\cdots$; LOMO-10 root signal.

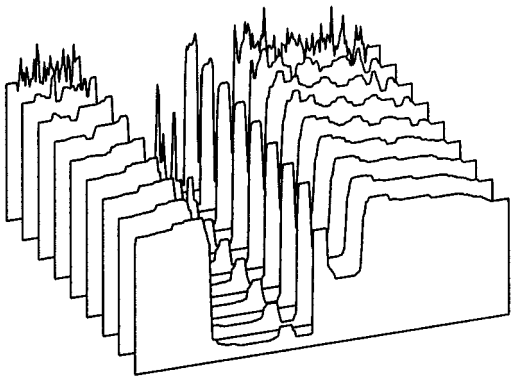

Fig. 4. Scale space generated by the median filter. From back to front: original noisy input signal ($N = 256$); LOMO-3 root signal; LOMO-4 root signal, $\cdots$; LOMO-10 root signal.

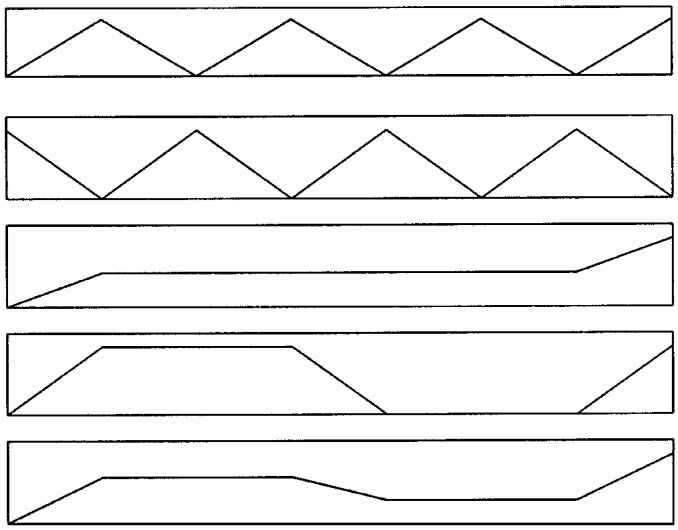

Fig. 5. From top to bottom. Input (oscillatory) signal; median filter (width 3) result (no root signal possible); LOMO-3 diffusion result (converged to root signal); LOMO-3 regression using L_1 norm; LOMO-3 regression using L_2 norm.

III. Analysis

In the analysis of LOMO diffusion, we will show that the range of the output signal is a subset of the range of the input signal. We will prove that LOMO diffusion enforces monotonicity on certain subsequences of the signal and that the diffusion operation converges to a root signal in a tightly bounded

number of iterations. It will be proven that the nested diffusion operations do not exhibit oscillatory behavior and that the diffusion coefficient used in LOMO diffusion is the sole possibility for generating a nontrivial LOMO signal. Finally, we consider a special case of LOMO diffusion that is identical to the LOMO regression: the optimal solution.

We provide a few observations that are needed for the analysis.

Observation 1: The LOMO diffusion update (see Definition 3) will leave a monotone point unchanged, unless the antilag term $a(x)$ in (14) is asserted. In the case where the antilag term is asserted, a monotone point will follow a neighboring point in order to remain monotone. Proof that LOMO diffusion will retain the monotone points can be given by inspection of the LOMO diffusion update when $\text{sgn}[\nabla I_w(x)] \neq \text{sgn}[\nabla I_e(x)]$. Since $\nabla I_w(x) \leftarrow -\nabla I_e(x)$ when $\nabla I_w(x) = 0$ and $\nabla I_e(x) \leftarrow -\nabla I_w(x)$ when $\nabla I_e(x) = 0$, $[I(x)]_{t+1} = [I(x)]_t$ in this case.

Observation 2: The LOMO diffusion update will decrement a positive-going nonmonotone point (by unity) and will increment a negative-going nonmonotone point unless the overshoot expression $l(x)$ in (11) is true for a OGSD point.

Observation 3: In the root signal $\boldsymbol{I} = ld(\boldsymbol{I}^0, h_w, h_e)$, for $h_e = h_w$, $I(x) = I(x - h_w)$ or $I(x) = I(x + h_e)$ for each point x that was nonmonotone in $\boldsymbol{I}^0$.

Proofs of Observations 2 and 3 can be given via examination of $(p/2)\{\text{sgn}[\nabla I_w(x)\}] + \text{sgn}[\nabla I_e(x)]\}$ in (8) when $\text{sgn}[\nabla I_w(x)] = \text{sgn}[\nabla I_e(x)]$. If $I(x)$ is a positive-going nonmonotone point and $l(x)$ is false in (11), $(p/2)\{\text{sgn}[\nabla I_w(x)] + \text{sgn}[\nabla I_e(x)]\} = -1$. If $I(x)$ is a negative-going nonmonotone point and $l(x)$ is false, $(p/2)\{\text{sgn}[\nabla I_w(x)] + \text{sgn}[\nabla I_e(x)]\} = 1$. From the definitions of nonmonotone points (Definition 2), monotonicity of $\{I(x - h_w), I(x), I(x + h_e)\}$ will be achieved when $I(x) = I(x - h_w)$ or $I(x) = I(x + h_e)$. When $I(x) = I(x - h_w)$ or $I(x) = I(x + h_e)$, (8) will not alter the two equal points in the case of $h_e = h_w$ because both are monotone, and $(p/2)\{\text{sgn}[\nabla I_w(x)] + \text{sgn}[\nabla I_e(x)]\} = 0$ [since $\nabla I_w(x) \leftarrow -\nabla I_e(x)$ when $\nabla I_w(x) = 0$ and $\nabla I_e(x) \leftarrow -\nabla I_w(x)$ when $\nabla I_e(x) = 0$ by Definition 3]. In addition, note that $l(x)$ in (11) prevents two related points that differ by one intensity level from passing each other.

First, we need to establish that the range of the LOMO diffusion operation is a subset of the range of the input signal. We do not want a PDE in which the output can stray from the original range.

Observation 4: Given input signal $\boldsymbol{I}$, $I(x) \in \boldsymbol{Z}$, $0 \leq I(x) \leq K - 1 \forall x$, if $\boldsymbol{J} = ld(\boldsymbol{I}, h_w, h_e)$, then $J(x) \in \boldsymbol{Z}$, and $0 \leq J(x) \leq K - 1 \ \forall x$.

Proof: Let $I^0(x) = I(x)$ and $J(x) = I^T(x)$ [which is an evolution of $I^0(x)$] for $T > 0$. First, we show that LOMO diffusion is closed under the integers. If $I^t(x) \in \boldsymbol{Z}$, then $I^{t+1}(x) \in \boldsymbol{Z}$ because in (8), the difference between $I^{t+1}(x)$ and $I^t(x)$ is $(p(x)/2)\{\text{sgn}[\nabla I_w(x)] + \text{sgn}[\nabla I_e(x)]\} + a(x) \in \{-1, 0, 1\} \subset \boldsymbol{Z}$. Note that when $a(x)$ is nonzero (-1 or 1), $(p(x)/2)\{\text{sgn}[\nabla I_w(x)] + \text{sgn}[\nabla I_e(x)]\}$ is zero. In addition, the term $p(x) \in \{0, 1\}$. Since the integers are closed under addition and $I^0(x) \in \boldsymbol{Z}$, then $I^T(x) \in \boldsymbol{Z}$, and $J(x) \in \boldsymbol{Z}$.

Now, we show that LOMO diffusion is bounded by the range of the input signal $\boldsymbol{I}$. Assume that $\boldsymbol{I}^t \in [0, K - 1]^N$ and that $I^{t+1}(x) < 0$ for some x. From (8), we observe that the maximum change between updates is $\max|(1/2)\{\text{sgn}[\nabla I_w(x)] + \text{sgn}[\nabla I_e(x)]\} + a(x)| = 1$. Therefore, $I^t(x) = 0$. By Observations 1 and 2, both of the following conditions must be true for a negative change in $I(x)$: $I^t(x) >_I^t (x - h_w)$ and $I^t(x) > I^t(x + h_e)$. Therefore, $I^t(x - h_w) < 0$, and $I^t(x + h_e) < 0$, which is a contradiction to $\boldsymbol{I}^t \in [0, K - 1]^N$. A similar contradiction can be established for the case where $I^{t+1}(x) > K - 1$. We conclude that $0 \leq J(x) \leq K - 1 \ \forall x$.

In examining the convergence behavior of LOMO diffusion, it is important to establish that LOMO diffusion will not change a positive-going nonmonotone point to a negative-going nonmonotone point and *vice versa*.

Observation 5: LOMO diffusion will not change a positive-going nonmonotone point to a negative-going nonmonotone point and *vice versa*.

Proof: We consider two cases: $h_e = h_w$ and $h_e \neq h_w$. For $h_e = h_w$, each nonmonotone point $I(x)$ will become equal to $I(x - h_w)$ or $I(x + h_e)$ and will then remain unchanged (see Observation 3). Therefore, a positive-going nonmonotone point cannot become a negative-going nonmonotone point and *vice versa*.

When $h_e \neq h_w$, $I(x - h_w)$ and $I(x + h_e)$ must "pass" $I(x)$ to make a positive-going nonmonotone into a negative-going nonmonotone point or *vice versa*. In the process, $I(x)$ will become equal to $I(x - h_w)$ or $I(x + h_e)$ and remain equal via the antilag term $l(x)$ in (14). Therefore, the transition from positive-going to negative-going or negative-going to positive-going is impossible.

Theorem 1 shows that LOMO diffusion forces the subsequence $\{I(x - h_w), I(x), I(x + h_e)\}$ to become monotonic in a bounded number of iterations.

Theorem 1: $ld(\boldsymbol{I}, h_w, h_e)$ converges to a signal in which each subsequence $\{I(x - h_w), I(x), I(x + h_e)\}$ is monotonic $\forall x$: $h_w \leq x \leq N - h_e - 1$ in a number of iterative steps bounded by $K - 1$ for a signal with K discrete intensity levels.

Proof: Again, we examine two cases, $h_e = h_w$ and $h_e \neq h_w$. With $h_e = h_w$, $I(x)$ and $I(x - h_w)$ cannot simultaneously increase or decrease because both points cannot be positive-going or negative-going by Definition 2. The same argument holds for $I(x)$ and $I(x + h_e)$. Therefore, if $I(x)$ is increasing, then $I(x - h_w) > I(x)$ and $I(x + h_e) > I(x)$, making $I(x - h_w)$ and $I(x + h_e)$ decreasing or constant. Each nonmonotone point will continue to change until equal in value to either $I(x - h_w)$ or $I(x + h_e)$, at which point, the equal values will remain unchanged. Note that the two neighbors cannot pass each other when the overshoot term $l(x)$ in (11) is applied. Thus, the worst case for the number of updates for position x is bound by the minimum of $|\nabla I_w(x)|$ and $|\nabla I_e(x)|$, which are bound above by $K - 1$.

The case of $h_e \neq h_w$ must be handled separately since $I(x - h_w)$ and $I(x)$ [and $I(x + h_e)$ and $I(x)$] are not codependent [*viz.*, $I(x - h_w)$ and $I(x)$ can be equal with $I(x - h_w)$ being nonmonotone]. If an $I(x)$ has $I(x - h_w)$ and $I(x + h_e)$ that are constant, then $I(x)$ does not change the direction of update and becomes monotone (via equality) in at most min $\{|\nabla I_w(x)|,$

$|\nabla I_e(x)|\}$ updates, which is bounded by $K-1$. The only case in which $I(x)$ can change directions of update is if $I(x-h_w)$ or $I(x+h_e)$ are changing in the opposite direction. Assume that $I(x-h_w)$ and $I(x+h_e)$ are originally negative-going nonmonotone points and thus increasing, whereas $I(x)$ is positive-going nonmonotone and decreasing. By Observation 5, $I(x)$ cannot "pass" $I(x-h_w)$ or $I(x+h_e)$ and become a negative-going nonmonotone point. In fact, when $I(x)$ becomes equal to $I(x-h_w)$, without loss of generality (W.L.O.G.), $I(x)$ will "follow" $I(x-h_w)$ via the antilag term in (14). Thus, the convergence of $I(x)$ will depend on the convergence of $I(x-h_w)$ in this case. If $I(x-h_w)$ depends on positive-going nonmonotone points $I(x-2h_w)$ and $I(x-h_w+h_e)$, then these points will govern the convergence of the interdependent group. Note that the maximum convergence time will always be $K-1$ steps since within an interdependent relationship, there will always be an $I(y)$ with constant $I(y-h_w)$ or $I(y+h_e)$ since the signal is finite and the boundary points are fixed for $y<h_w$ and $y>N-h_e-1$.

For both $h_e=h_w$ and $h_e\neq h_w$, when $\boldsymbol{I}$ has converged and each $I(x)$ is unchanged, $\boldsymbol{I}$ contains no nonmonotone points, and $\{I(x-h_w),\, I(x),\, I(x+h_e)\}$ is monotonic $\forall x$: $h_w\leq x\leq N-h_e-1$.

Given an input signal with K intensity levels, the worst-case overall number of iterations needed for convergence to a root signal is $K-1$. This $O(K)$ convergence time holds for LOMO signals of varying degrees (see experimental results in Section IV). Consequently, the convergence time is not dependent on the signal length but on the quantization of the discrete signal.

Furthermore, the choice of the diffusion coefficient is not arbitrary, as shown by Theorem 2.

Theorem 2: For anisotropic diffusion using (2), diffusion coefficients of the form of (6) uniquely allow LOMO-d ($d\geq 3$) root signals.

Proof: The lomotonicity of a signal may be evaluated from the sign skeleton of its difference signal alone $S(x)$. If the length-3 segment centered at location x in $\boldsymbol{I}$ is not monotone, then $I(x)$ is a nonmonotone point for ($h_w=h_e=1$) and $\text{sgn}[\nabla I_w(x)]=\text{sgn}[\nabla I_e(x)]$. By Observation 2, $I(x)$ will be changed by LOMO diffusion. When $I(x)$ is a monotone point, it will remain unchanged (by Observation 1). Thus, LOMO-d ($d\geq 3$) signals are root signals of LOMO diffusion. Assume $\text{sgn}[\nabla I_w(x)]\neq\text{sgn}[\nabla I_e(x)]$, and consider two cases: $\nabla I_w(x)=-\nabla I_e(x)+\varepsilon$ and $\nabla I_w(x)=-\nabla I_e(x)-\varepsilon$ [where $\varepsilon>0$]. Using (2), we assert that

$$c_e(x)\nabla I_e(x)=c_w(x)\nabla I_w(x) \tag{17}$$

for $I(x)$ to remain unchanged. Combining the two cases, we have

$$\begin{aligned} &c\left[|\nabla I_w(x)-\varepsilon|\right]\left[-\nabla I_w(x)+\varepsilon\right]\\ &\quad=c\left[|\nabla I_w(x)+\varepsilon|\right]\left[-\nabla I_w(x)-\varepsilon\right] \end{aligned} \tag{18}$$

where $c(|g|)$ is the diffusion coefficient for a gradient magnitude of $|g|$. Under the stated assumptions for the diffusion coefficient (smooth nonincreasing functions of $|g|$), the only solutions to (18) are diffusion coefficients of the form $c_p(x)=(\kappa)/(|\nabla I_p(x)|)$ (for $\kappa>0$). Therefore, only LOMO diffusion will leave the length-3 (or greater) monotonic subsequences unchanged. By Observation 2, non-LOMO-3 signals will be changed by LOMO diffusion, and thus, LOMO-3 signals are root signals. LOMO-d signals are also root signals, where $d>3$ since every signal that is LOMO-a is also LOMO-b if $a\geq b$.

Hence, Theorem 2 shows that the diffusion coefficient used in LOMO diffusion uniquely provides LOMO fixed points. As a consequence, we can assert that LOMO-(h_w+h_e+1) signals are fixed points of $ld(\boldsymbol{I},\, h_w,\, h_e)$. This is easily proven because $ld(\boldsymbol{I},\, h_w,\, h_e)$ will not alter signals that are LOMO-(h_w+h_e+1) (see Observations 1 and 2). Note that this result does not preclude a fixed point for non-LOMO-(h_w+h_e+1) signals. Obviously, subsequent diffusions are required to generate the LOMO-(h_w+h_e+1) root signals [see (15) and (16)].

Theorem 2 shows that LOMO-d signals are roots of LOMO diffusion $ld_d(\boldsymbol{I})$. The complementary question follows: Do roots of $ld_d(\boldsymbol{I})$ exist that are not LOMO-d? To show that these non-LOMO root signals are impossible, let us assume that a signal $\boldsymbol{J}_2=ld_4(\boldsymbol{I})$ that is not LOMO-4 (since the LOMO-3 case is trivial) exists. In the process of computing $ld_4(\boldsymbol{I})$, we have the first step $\boldsymbol{J}_1=ld(\boldsymbol{I},\,1,\,2)$ and the second step $\boldsymbol{J}_2=ld(\boldsymbol{J}_1,\,1,\,1)$, following (16). We know that $\boldsymbol{J}_2=ld(\boldsymbol{J}_1,\,1,\,1)$ is LOMO-3; therefore, for $\boldsymbol{J}_2$ to be non-LOMO-4, there exists an x such that $J_2(x)>J_2(x+2)$ and $J_2(x)>J_2(x-1)$, assuming $J_2(x)$ is a positive going nonmonotone point, W.L.O.G. Therefore, $ld(\boldsymbol{J}_1,\,1,\,1)$ had to change either $J_1(x)$, $J_1(x+2)$, or $J_1(x-1)$. The operation $ld(\boldsymbol{J}_1,\,1,\,1)$ could not change $J_1(x+2)$ to become less than $J_1(x)$ because $J_2(x+1)=J_2(x)$ and $J_1(x+2)$ would have to "pass" $J_1(x+1)$ in this case. Similarly, $ld(\boldsymbol{J}_1,\,1,\,1)$ would not change $J_1(x-1)$ to become less than $J_1(x)$; they would become equal if $J_1(x-1)$ were decreased. In this scenario, since $J_2(x+1)\geq J_2(x-1)$, if $J_1(x)$ were a negative-going nonmonotone point w.r.t. $ld(\boldsymbol{J}_1,\,1,\,1)$, $J_1(x)$ would become equal to $J_1(x-1)$, which would not violate the monotonicity relationship of $ld(\boldsymbol{I},\,1,\,2)$. Therefore, the non-LOMO-4 signal is impossible. In this manner, the preclusion of non-LOMO root signals can be likewise extended to higher degrees of local monotonicity.

The preceding analysis examines the generation of locally monotonic signals from LOMO diffusion. We have not discussed, however, the closeness between the input and output signals. A locally monotonic result that minimizes the distance between the input signal and the LOMO result is a LOMO regression. We can show that a special case of LOMO diffusion $ld_3(\boldsymbol{I})$ leads to a LOMO-3 regression, which is the optimal result.

Theorem 3: $\boldsymbol{R}=ld_3(\boldsymbol{I})$ gives a digital LOMO-3 regression for $\boldsymbol{I}$ under the L_1 norm.

Proof: To prove that $\boldsymbol{R}$ is a digital LOMO-3 regression for $\boldsymbol{I}$ under the L_1 norm, it suffices to prove that there does not exist a LOMO-3 signal $\boldsymbol{S}$, $S(x)\in\boldsymbol{Z}$ such that

$$\sum_{x=0}^{N-1}|S(x)-I(x)|<\sum_{x=0}^{N-1}|R(x)-I(x)|. \tag{19}$$

For each x where $|S(x)-I(x)| < |R(x)-I(x)|$ and $|S(x)-I(x)| = |R(x)-I(x)| + \alpha$, if

$$|S(x)-I(x)| + |S(x+1)-I(x+1)| \geq |R(x)-I(x)| + |R(x+1)-I(x+1)| \quad (20)$$

or

$$|S(x)-I(x)| + |S(x-1)-I(x-1)| \geq |R(x)-I(x)| + |R(x-1)-I(x-1)| \quad (21)$$

then $\sum_{x=0}^{N-1} |S(x)-I(x)| \geq \sum_{x=0}^{N-1} |R(x)-I(x)|$, and (19) does not hold.

Where $|S(x)-I(x)| < |R(x)-I(x)|$, there are two cases: a) LOMO diffusion "passed" the value $S(x)$ [using initial guess $I(x)$], and b) LOMO diffusion updated $R(x)$ in the "wrong direction." For case a), W.L.O.G., assume $I(x) > I(x-1)$ and $I(x) > I(x+1)$. Then, in case a), $R(x) < S(x)$ and $S(x) \leq I(x)$, given that $|S(x)-I(x)| < |R(x)-I(x)|$. By Observation 3, $R(x) = \max\{R(x-1), R(x+1)\}$ and $R(x-1) \leq R(x), R(x+1) \leq R(x)$. Since $\boldsymbol{S}$ is LOMO-3, either $S(x-1) \leq S(x) \leq S(x+1)$ or $S(x-1) \geq S(x) \geq S(x+1)$ holds. By assumption $R(x) < S(x)$, and either $R(x-1) < S(x-1)$ or $R(x+1) < S(x+1)$. Let $S(x) = R(x) + \beta$ so that $R(x-1) + \beta \leq S(x-1)$ or $R(x+1) + \beta \leq S(x+1)$, which asserts either (20) or (21).

In case b), we again assume that $I(x) > I(x-1)$ and $I(x) > I(x+1)$. This time, $R(x) < S(x)$ and $S(x) \geq I(x)$ since, by Observation 2, $R(x) \leq I(x)$. Let $S(x) - I(x) = \alpha$ and $I(x) - R(x) = \beta$, where $\alpha, \beta \geq 0$. Since $\boldsymbol{S}$ is LOMO-3, either $S(x-1) \leq S(x) \leq S(x+1)$ or $S(x-1) \geq S(x) \geq S(x+1)$. Therefore, either $S(x-1) > I(x-1)$ and $S(x-1) \geq S(x)$ or $S(x+1) > I(x+1)$ and $S(x+1) \geq S(x)$. Therefore, either $S(x-1) - I(x-1) \geq \alpha + \beta$ or $S(x+1) - I(x+1) \geq \alpha + \beta \geq \beta - \alpha$ so that (20) or (21) holds, which precludes (19). $\boldsymbol{R}$ is a digital LOMO-3 regression for $\boldsymbol{I}$ under the L_1 norm.

Note that an optimal LOMO result in the mathematical sense, which is a LOMO regression, may be undesirable. Consider the LOMO-3 regressions under the L_1 and L_2 norms shown in Fig. 5. These results were generated using the algorithms in [10]. The interpretation given by LOMO diffusion is arguably more intuitive (see Fig. 5). The PDE-based method that evolves the original signal appears to preserve important signal trends and retain the structure of the signal.

A main goal in pursuing LOMO diffusion is the generation of scale-space representations that can be used in content-based retrieval and hierarchical search processes. We can observe that LOMO diffusion provides a causal scale space. This means that no new features are created with increasing scale. Let scale be represented by lomotonicity of the signal and not by the traditional notion of diffusion time. A new feature is created if a new signal edge is introduced. Consider a LOMO-$(d-1)$ signal and a LOMO-d signal generated by LOMO diffusion. For a new signal edge to be introduced, one of the following must be true within a d-length interval of the LOMO-d signal.

1) The gradient magnitude must change from zero at a point to a nonzero value (a constant interval becomes nonconstant).
2) The gradient must change from positive to negative in direction (an increasing interval becomes decreasing locally).
3) The gradient must change from negative to positive (a decreasing interval becomes increasing).

Otherwise, if the gradient is the same, no new edge is introduced. Case 1 is clearly impossible in LOMO diffusion because a constant sequence will not be changed (see Observation 1). Cases 2 and 3 are also impossible, as LOMO diffusion will never change an increasing sequence to a decreasing sequence, nor will it change a decreasing sequence to an increasing sequence (see Observation 5). The only possibility is the change of an increasing/decreasing subsequence within an interval to a constant subsequence. Therefore, we can conclude that LOMO diffusion does provide a causal scale space.

As mentioned, the median filter also produces LOMO root signals and can be used to generate a scale-space representation as in Fig. 4. The results from the literature can be summarized by Theorem 4.

Theorem 4 [6], [13]: The output of a length $w = 2m+1$ median filter median $(\boldsymbol{I})$ equals $\boldsymbol{I}$ if and only if $\boldsymbol{I}$ is LOMO-$(m+2)$. Suppose that the signal $\boldsymbol{I}$ contains at least one monotonic segment of length $m+1$. Then, the $w = 2m+1$ median filter will reduce a length-N signal to a root signal that is LOMO-$(m+2)$ in at most $(N-2)/2$ repeated passes.

From Theorem 4, we can observe that the median filter will require a significant number of iterations to reach the root signal on long signals. In addition, a restriction is placed on the initial signal; it must contain a monotonic subsequence. With LOMO diffusion, the convergence to a root is not dependent on the length of the signal, and LOMO diffusion will produce a LOMO signal of the desired degree regardless of the input signal (see Fig. 5). The quality and cost associated with the median filter will be contrasted with that of LOMO diffusion in Section IV.

IV. Results and Conclusions

In the empirical study, we selected 100 unique signals of length $N = 256$ from a database of signals acquired via an optical scanner. Tables I and II provide a comparison between the performance of LOMO diffusion and that of the median filter on the 100 uncorrupted signals. An example signal is given in Fig. 6. The median result of Fig. 6 is LOMO (of degree $d = 4$), as is the LOMO-4 diffusion result. Using the same number of updates, the standard anisotropic diffusion algorithm is not able to remove features of small scale. Tables III and IV provide the results obtained when the experiments were repeated for noisy data. The signals were corrupted by Laplacian-distributed additive noise (SNR $=$ 10 dB, standard deviation $\sigma = 10.0$) in this case. Fig. 7 repeats the example of Fig. 6 for the noisy case. The standard anisotropic diffusion algorithm is not able to eradicate the impulses from the noise. The only perceivable (qualitative) difference between the median filter result in Fig. 7 and the LOMO diffusion result in Fig. 7 is that LOMO diffusion retains the sharpness of the signal transitions, and the median filter tends to "round" the edges.

One general conclusion from the experiments is that LOMO diffusion provides a signal of equal or higher lomotonicity and

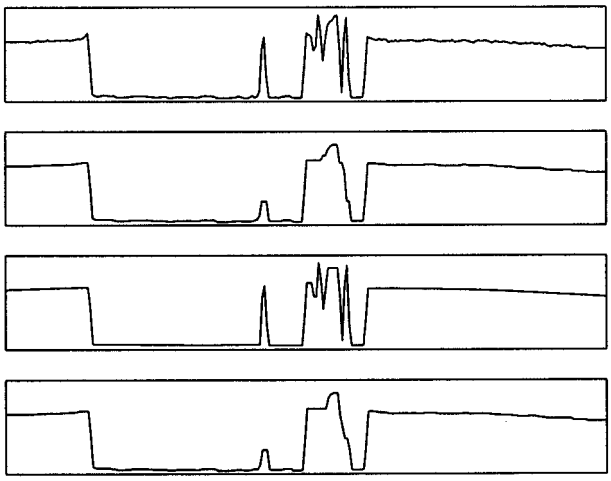

Fig. 6. From top to bottom: Original signal ($N = 256$); median root (LOMO-4); 150 iterations of the standard diffusion algorithm using (5) with $k = 10$; 150 iterations of LOMO-4 diffusion.

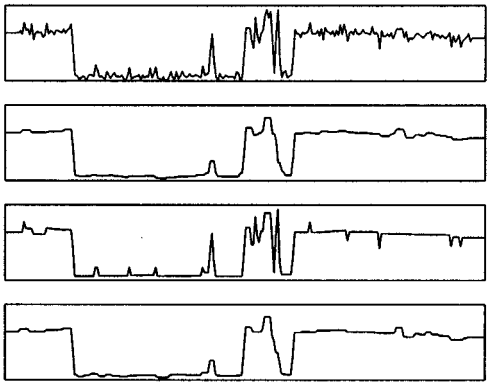

Fig. 7. From top to bottom: Original signal ($N = 256$) corrupted with Laplacian noise; median root (LOMO-4); 150 iterations of the standard diffusion algorithm using (5) with $k = 10$; 150 iterations of LOMO-4 diffusion.

equivalent mean absolute error (MAE) compared with the median roots. With the corrupted signals, both the diffusion method and the median filter are able to remove outliers and denoise the signals. Unlike current diffusion techniques that either retain outliers or utilize additional filtering processes to enhance diffusion, LOMO diffusion is able to eradicate the noise without additional filtering. However, the LOMO diffusion operation is far less costly than repeated application of the median filter.

Tables I and II provide the average number of operations used in generating a LOMO diffusion root signal and the number of operations used to compute a median root signal. We assume that a comparison operation has the same computational complexity as an integer addition/subtraction. A binary shift (for division by two) is also assumed to have the same complexity. Under these assumptions, seven operations are expended for each LOMO diffusion iteration per pixel. Implementing the median filter in the standard sorting scheme, $\sum_{i=(w-1)/2}^{w} i$ comparison operations are used for a w-width filter on one pixel. We have not accounted for more expeditious median filter schemes, as in [2] and [7]. Although the assumptions used in the complexity analysis may be argued, the difference between the costs is stark. For LOMO degrees above 10, the difference in the number of operations needed exceeds an order of magnitude. Clearly, it is advantageous computationally to use LOMO diffusion when the desired degree of lomotonicity is greater than 3.

We are currently exploring 2-D extensions for LOMO diffusion. The most straightforward extension of (7) is to implement the following update on each image pixel:

$$[I(x)]_{t+1} \leftarrow \left(I(x) + (\Delta T) \left\{ \begin{array}{l} \operatorname{sgn}[\nabla I_w(x)] \\ \quad + \operatorname{sgn}[\nabla I_e(x)] \\ \quad + \operatorname{sgn}[\nabla I_n(x)] \\ \quad + \operatorname{sgn}[\nabla I_s(x)] \end{array} \right\} \right)_t \tag{22}$$

with time step $\Delta T \leq (1/4)$. The additional terms $\nabla I_n(x)$ and $\nabla I_s(x)$ are the signal differences in the "northern" and "southern" diffusion directions, respectively. We call (22) *the full 2-D extension*. Another 2-D extension is realized by applying 1-D LOMO diffusion in the image direction orthogonal to the gradient. This method, which bears similarity to the mean curvature motion implementations of 2-D diffusion, is called the *direct 2-D extension*. To demonstrate the application of LOMO diffusion to image processing, the 256×256 image shown in Fig. 8 has been corrupted with additive Laplacian-distributed noise, as shown in Fig. 9. Fig. 10 displays the result of the full 2-D extension of LOMO diffusion, whereas Fig. 11 shows the result of applying the direct 2-D extension. Both 2-D enhancement methods are able to eliminate the heavy-tailed noise and preserve important features in the image. Qualitatively, we observe that the full extension is superior in retaining details (such as in the cameraman's face), whereas the direct method excels in preserving linear features (such as the colonnade). In contrast, the standard anisotropic diffusion algorithm [9] cannot remove the signal outliers, as shown in Fig. 12. Attempting to remove the noise via regularized diffusion [5] with a Gaussian-smoothed gradient estimate results in oversmoothing and feature degradation, as shown in Fig. 13. In future work, we plan to extend the theoretical results given in Sections II and III of this paper to the multidimensional LOMO diffusion case.

A PDE-based method to generate LOMO signals has been developed and analyzed. Compared with previous diffusion techniques that converge to constant or piecewise constant signals, the LOMO diffusion method converges to nontrivial signals of the desired scale. The lomotonicity of the signal allows a description of signal smoothness for digital signals and parameterizes a useful signal scale space. From the analysis, we can conclude that LOMO diffusion is well behaved and converges rapidly and independently of the number of signal samples. LOMO diffusion does not require ambiguous parameters and does not preserve impulse noise.

TABLE I
RESULTS FROM LOMO-d DIFFUSION ON 100 SIGNALS OF LENGTH $N = 256$

Minimum Lomotonicity (d)	Average Lomotonicity	Average MAE	Average Number of Iterations for Root Signal	Average Number of Operations Per Signal
3	3.0	1.9	110.6	198,195
4	4.0	3.7	113.5	203,392
5	5.0	5.0	174.1	311,987
6	6.0	6.3	163.9	293,708
7	7.0	7.2	236.7	424,166
8	8.1	8.4	171.7	307,686
9	9.5	9.7	278.0	498,176
10	10.5	10.1	190.4	341,197

TABLE II
RESULTS FROM COMPUTING MEDIAN ROOT SIGNALS OF 100 SIGNALS OF LENGTH $N = 256$ ($d = m + 2$ IN THEOREM 4)

Minimum Lomotonicity (d)	Average Lomotonicity	Average MAE	Iterations for Root Signal	Width (w)	Number of Operations Per Signal
3	3.0	2.0	127	3	162,560
4	4.0	4.1	127	5	390,144
5	5.0	5.5	127	7	715,264
6	6.0	6.4	127	9	1,137,920
7	7.0	7.1	127	11	1,658,112
8	8.0	8.4	127	13	2,275,840
9	9.2	9.5	127	15	2,991,104
10	10.2	10.3	127	17	3,803,904

TABLE III
RESULTS FROM LOMO-d DIFFUSION ON 100 SIGNALS OF LENGTH $N = 256$ CORRUPTED WITH LAPLACIAN-DISTRIBUTED NOISE

Minimum Lomotonicity (d)	Average Lomotonicity	Average MAE	Average Number of Iterations for Root Signal	Average Number of Operations Per Signal
3	3.0	7.4	114.3	204,826
4	4.0	11.1	118.8	212,889
5	5.0	13.0	182.2	326,502
6	6.1	14.6	172.9	309,836
7	7.1	16.0	247.6	443,699
8	8.4	17.1	199.3	357,145
9	10.5	18.5	293.5	525,952
10	12.4	18.9	228.6	409,651

TABLE IV
RESULTS FROM COMPUTING MEDIAN ROOT SIGNALS ON 100 SIGNALS OF LENGTH $N = 256$ CORRUPTED WITH LAPLACIAN-DISTRIBUTED NOISE ($d = m + 2$ IN THEOREM 4)

Minimum Lomotonicity (d)	Average Lomotonicity	Average MAE	Iterations for Root Signal	Width (w)	Number of Operations Per Signal
3	3.0	8.2	127	3	162,560
4	4.0	11.9	127	5	390,144
5	5.0	13.7	127	7	715,264
6	6.0	14.8	127	9	1,137,920
7	7.0	15.7	127	11	1,658,112
8	8.0	16.8	127	13	2,275,840
9	9.1	17.7	127	15	2,991,104
10	10.3	18.7	127	17	3,803,904

Fig. 8. Original cameraman image.

Fig. 9. Cameraman image corrupted by Laplacian noise (SNR $= 13$ dB).

Fig. 10. Two-dimensional LOMO diffusion result by full 2-D extension (degree $d = 3$).

Fig. 11. Two-dimensional LOMO diffusion result by direct 2-D extension (degree $d = 3$).

Fig. 12. Standard anisotropic diffusion using (5) for the diffusion coefficient.

Fig. 13. Anisotropic diffusion with Gaussian prefilter in the diffusion coefficient.

REFERENCES

[1] S. T. Acton, "Diffusion-based edge detectors," in *Image and Video Processing Handbook*, A. C. Bovik, Ed. New York: Academic, 1999.

[2] J. T. Astola and T. G. Campbell, "On computation of the running median," *IEEE Trans. Acoust., Speech, Signal Processing*, vol. 37, pp. 572–574, Feb. 1989.

[3] M. J. Black, G. Sapiro, D. H. Marimont, and D. Heeger, "Robust anisotropic diffusion," *IEEE Trans. Image Processing*, vol. 7, pp. 421–432, Apr. 1998.

[4] V. Caselles, J.-M. Morel, G. Sapiro, and A. Tannenbaum, "Introduction to the special issue on partial differential equations and geometry-driven diffusion in image processing and analysis," *IEEE Trans. Image Processing*, vol. 7, pp. 269–273, Mar. 1998.

[5] F. Catte, P.-L. Lions, J.-M. Morel, and T. Coll, "Image selective smoothing and edge detection by nonlinear diffusion," *SIAM J. Numer. Anal.*, vol. 29, pp. 182–193, 1992.

[6] N. C. Gallagher and G. L. Wise, "A theoretical analysis of the properties of median filters," *IEEE Trans. Acoust., Speech, Signal Processing*, vol. ASSP-29, pp. 1136–1141, Dec. 1981.

[7] T. S. Huang, G. J. Yang, and G. Y. Tang, "A fast two-dimensional median filtering algorithm," *IEEE Trans. Acoust., Speech, Signal Processing*, vol. 27, pp. 13–18, Jan. 1981.

[8] J. D. Murray, *Mathematical Biology*. Berlin, Germany: Springer-Verlag, 1993.

[9] P. Perona and J. Malik, "Scale-space and edge detection using anisotropic diffusion," *IEEE Trans. Pattern Anal. Machine Intell.*, vol. 12, pp. 629–639, Apr. 1990.

[10] A. Restrepo (Palacios) and A. C. Bovik, "Locally monotonic regression," *IEEE Trans. Signal Processing*, vol. 41, pp. 2796–2810, Oct. 1993.

[11] C. A. Segall and S. T. Acton, "Morphological anisotropic diffusion," in *Proc. IEEE Int. Conf. Image Process.*, Santa Barbara, CA, Oct. 26–29, 1997.

[12] N. Sidiropoulos, "Fast digital locally monotonic regression," *IEEE Trans. Signal Processing*, vol. 45, pp. 389– 395, Feb. 1997.

[13] S. G. Tyan, "Median filtering: Deterministic properties," *Two-Dimensional Signal Processing: Transforms and Median Filters*, 1981.

[14] A. P. Witkin, "Scale-space filtering," in *Proc. Int. Joint Conf. Artif. Intell.*, 1983, pp. 1019–1021.

[15] A. Yezzi Jr., "Modified curvature motion for image smoothing and enhancement," *IEEE Trans. Image Processing*, vol. 7, pp. 345–352, Feb. 1998.

[16] Y.-L. You, W. Xu, A. Tannenbaum, and M. Kaveh, "Behavioral analysis of anisotropic diffusion in image processing," *IEEE Trans. Image Processing*, vol. 5, pp. 1539–1553, Dec. 1996.

Scott T. Acton (SM'99) received the B.S. degree in electrical engineering from Virginia Tech, Blacksburg, in 1988 and the M.S. and Ph.D. degrees, both in electrical engineering, from the University of Texas, Austin, in 1990 and 1993, respectively.

He has worked in industry for AT&T, the MITRE Corporation, and Motorola, Inc. Currently, he is an Associate Professor with the School of Electrical and Computer Engineering, Oklahoma State University, Stillwater, where he directs the Oklahoma Imaging Laboratory. The laboratory is sponsored by several organizations including NASA, the Army Research Office (ARO), and Lucent Technologies. His research interests include multiscale signal representations, diffusion algorithms, morphology, image restoration, image segmentation, and content-based retrieval.

Dr. Acton received the 1996 Eta Kappa Nu Outstanding Young Electrical Engineer Award, which is a national award that has been given annually since 1936. At OSU, he was selected as the 1997 Halliburton Outstanding Young Faculty Member. He serves as Associate Editor of the IEEE TRANSACTIONS ON IMAGE PROCESSING and is an active participant in the IEEE, SPIE, and Eta Kappa Nu.